



HAL
open science

Optimal control of a deep-towed vehicle by optimization techniques

Laurent Chauvier, Gilbert Damy, Jean Charles Gilbert, Nicolas Pichon

► To cite this version:

Laurent Chauvier, Gilbert Damy, Jean Charles Gilbert, Nicolas Pichon. Optimal control of a deep-towed vehicle by optimization techniques. Oceans'98, Sep 1998, Nice, France. pp.1634-1639, 10.1109/OCEANS.1998.726365 . hal-04142351

HAL Id: hal-04142351

<https://inria.hal.science/hal-04142351>

Submitted on 26 Jun 2023

HAL is a multi-disciplinary open access archive for the deposit and dissemination of scientific research documents, whether they are published or not. The documents may come from teaching and research institutions in France or abroad, or from public or private research centers.

L'archive ouverte pluridisciplinaire **HAL**, est destinée au dépôt et à la diffusion de documents scientifiques de niveau recherche, publiés ou non, émanant des établissements d'enseignement et de recherche français ou étrangers, des laboratoires publics ou privés.



Distributed under a Creative Commons Attribution - NonCommercial - NoDerivatives 4.0 International License

Optimal control of a deep-towed vehicle by optimization techniques

L. Chauvier[†], G. Damy[‡], J.Ch. Gilbert[†], and N. Pichon[‡]

June 21, 1998 (new typesetting on June 26, 2023)

Abstract

We consider the problem of controlling a subsea vehicle used to investigate the ocean floor and focus on deep-ocean systems deployed through a cable several thousand meters long. The objective is to evolve optimized orders to be sent to the bridge or directly to the ship dynamic positioning system in order to minimize the duration of non productive maneuvers. Various constraints acting on the vehicle can be expressed such as minimum altitude, maximum velocity, etc. An optimization algorithm has been developed, which may take such inequality constraints acting on the system state variables into account.

1 Introduction

Tethered vehicles are commonly used to investigate the sea-bottom or objects lying on it. They belong to two main categories: towed vehicles (either passive or controlled through steerable fins) and ROVs. At a depth ranging between 1000 and 6000 m, ROVs can no longer be operated directly from the surface through a roughly buoyant umbilical. Instead, they are deployed using a weighty intermediate body suspended from the surface through the main cable. The dynamic behavior of this body is nevertheless similar to that of towed vehicles in that their position is only controlled through winch action and surface support maneuvering.

Operating deep systems is specifically difficult and time consuming because the towing speed is practically limited to 2-2.5 knots, the response to ship maneuvers involves quite long delays (for example, a 3000 m long cable and weight system initially deployed vertically takes around two hours to reach a steady state towing configuration at 2 knots), and the horizontal distance between vessel and towed body typically equals the immersion (at 2 knots).

Until recently, deep tethered vehicles (sometimes called “fish” below) were essentially used to perform scientific studies of the sea-bottom and expertise of wrecks with military or historical interest. Deep surveys are now performed in relation with the exploitation of deep oilfields and telecom optical cable laying operations. To guarantee the safety of human groups, routine surveys might be performed to detect sediment instabilities on continental margins and slopes and to monitor the evolution of active submarine seismic structures. In this context, a higher attention is given to systems productivity. This can be achieved through a more efficient control of the towfish position.

A first attempt to evolve optimized orders to the bridge using a research algorithm is reported in [7]. A software was developed to determine the ship’s course to ensure that the towed vehicle will pass within a minimum distance from a specified target. In [5], the problem of

inverting the cable dynamics to make the towfish follow a prescribed trajectory is considered. More recently, Pichon [8] addressed the optimal control problem of finding a vessel trajectory bringing the vehicle from a given position to another one in a minimum time. The final state inequality constraints were taken into account by means of a penalization technique. However, the determination of adequate values for the various weighting coefficients was a delicate task. Therefore, it appeared necessary to use an optimization tool where the inequality constraints acting on the state variables could be handled in a more efficient manner.

The work presented in this paper also deals with the minimum time deep-towed vehicle control problem. To be able to tackle more difficult situations, we have developed a new optimization algorithm, in the class of nonlinear interior point methods (see [2, 3]), which has the potentiality to solve problems with many inequality constraints. In the present case, such constraints can be related to a required position at the end of a maneuver or to the presence of natural obstacles, such as the relief of the sea bed.

The paper is organized as follows. In section 2, we describe the towfish-cable model, which allows for winding and unwinding actions on the cable. The discretization in space (using a variational technique) and in time (by the BDF scheme) is discussed in section 3. In section 4, we briefly explain the numerical optimization method and discuss the results obtained with this new approach in section 5. We conclude in section 6.

2 Modelization of the problem

2.1 The cable-vehicle system

Let us first precise some notation. The model uses the following constants

g ,	gravitational acceleration,
ℓ ,	total length of the cable,
m_c ,	cable mass (w.r.t. water) per unit length,

[†]INRIA Rocquencourt, BP 105, 78153 Le Chesnay Cedex, France, Laurent.Chauvier@inria.fr, Jean-Charles.Gilbert@inria.fr (corresponding author).

[‡]IFREMER, Centre de Brest, BP 70, 29280 Plouzané, France, Gilbert.Damy@ifremer.fr.

c_t, c_n , cable drag coefficients,
 m_f , vehicle mass (w.r.t. water),
 c_h, c_z , vehicle drag coefficients

and the following independent variables

$s \in [0, \ell]$, curvilinear coordinate,
 $t \in \mathbb{R}$, time.

The cable-vehicle system is completely described by

$u(t) \in \mathbb{R}^3$, vessel position,
 $y(s, t) \in \mathbb{R}^3$, cable position w.r.t. the vessel,
 $T(s, t) \in \mathbb{R}$, tension in the cable.

The derivatives of a function $z(s, t)$ are denoted by

$$\dot{z}(s, t) = \frac{\partial z}{\partial t}(s, t) \quad \text{and} \quad z'(s, t) = \frac{\partial z}{\partial s}(s, t),$$

while $|\cdot|$ stands for the Euclidean norm in \mathbb{R}^3 .

We use a model already considered by other authors, see [4, 6] for example. The cable position y and the tension T satisfy, for all $s \in]0, \ell[$ and $t \in]0, t_{\max}[$,

$$m_c \ddot{y} - (Ty)' = d_c + m_c (g - \ddot{u}) \quad (2.1a)$$

$$|y'| = 1. \quad (2.1b)$$

Equation (2.1a) results from Newton's law of motion for an infinitely flexible cable. The hydrodynamic drag force per unit length d_c acting on the cable is given by $d_c = -c_t |v_t| v_t - c_n |v_n| v_n$, where v_t and v_n are the tangential and normal components of the cable speed (both depend on \dot{y} , \dot{u} and y'). We assume that the cable is inextensible, which is expressed by (2.1b). The tension can then be viewed as a multiplier associated with this constraint.

The evolution partial differential equations (2.1) first need boundary conditions. For all $t \in]0, t_{\max}[$,

$$y(\ell, t) = 0 \quad (2.2a)$$

$$m_f \ddot{y}(0, t) = (Ty')(0, t) + d_f + m_f (g - \ddot{u}(t)). \quad (2.2b)$$

Equation (2.2a) means that the cable is fixed to the vessel, while (2.2b) is Newton's law, applied here to the vehicle. The drag force $d_f = -c_h |v_h| v_h - c_z |v_z| v_z$ depends on v_h and v_z , the horizontal and vertical components of the vehicle velocity. Our model also needs initial conditions for the position of the cable. For all $s \in]0, \ell[$,

$$y(s, 0) = y_0(s) \quad \text{and} \quad \dot{y}(s, 0) = v_0(s), \quad (2.3)$$

where y_0 and v_0 are the given initial position and speed of the cable w.r.t. the ship. There are neither boundary conditions nor initial conditions for the tension.

2.2 Variable length cables

In practice, it may be interesting to wind or unwind the cable from the ship deck to speed up a maneuver. We show in this section how to adapt the model above to take this possibility into account. We denote by $\ell(t)$ the

length of the immersed part of the cable at time t . It is clear that the dynamics of the system is still described by (2.1), but now for $s \in]0, \ell(t)[$. The fact that the length of the cable may change and the dynamics linked to this are simply expressed by modifying the boundary condition (2.2a), which becomes: for all $t \in]0, t_{\max}[$

$$y(\ell(t), t) = 0. \quad (2.4)$$

The initial conditions (2.3) now hold for $s \in]0, \ell(0)[$.

A possible strategy to solve this new model is to express the cable dynamics on the constant interval $[0, 1]$, thanks to the change of variable $\hat{s} = s/\ell(t)$. The resulting equations could then be integrated in space on $[0, 1]$. However, their nature may depend on how fast $\ell(t)$ varies with t . Furthermore, the stability of the discretized equations may also be influenced by the cable winding. For these reasons we have preferred another technique, which preserves the structure of equations (2.1) and has the advantage of being easier to implement.

Let ℓ_{\max} denote the maximum length of the cable, so that $\ell(t)$ must be taken in $]0, \ell_{\max}[$. In our approach, we integrate equations (2.1) not only on $]0, \ell(t)[$, but on $]0, \ell_{\max}[$. To realize condition (2.4), we leave free the upper end of the cable (for $s = \ell_{\max}$) and impose the boundary condition

$$y(\ell_{\max}, t) = \kappa(t),$$

where κ is an unknown function. Roughly speaking, at any time, the new system has one more unknown ($\kappa(t) \in \mathbb{R}^3$) and one more equation ((2.4) with values in \mathbb{R}^3 also). Numerical experiments have shown that it is as easy to solve as the previous model. Of course, we are finally only interested in $y(s, t)$, for $s \in]0, \ell(t)[$.

2.3 Optimization of the vessel displacement

We can now formulate the minimum time deep-towed vehicle control problem. The state variables are y , \dot{y} , T , and κ and the control parameters are \dot{u} , t_{\max} , and ℓ . The aim is to minimize the total time t_{\max} , while preserving certain constraints.

The state equations (2.1), (2.2), and (2.3) (with the appropriate changes discussed in section 2.2) are viewed as equality constraints for the minimization problem.

We also consider inequality constraints on the state and control variables. Here are some examples. The final position of the cable has to belong to the tube of radius $r_y > 0$ defined by $|y(\cdot, t_{\max}) - \tilde{y}(\cdot)| \leq r_y$, where \tilde{y} is some prescribed final position. Similar constraints can be given on the final speed of the cable. Also, to take care of the relief of the sea bed, the vehicle altitude $y_3(0, \cdot)$ has to be above a certain surface given by a function φ . This constraint can be expressed by $\varphi(y_1(0, \cdot), y_2(0, \cdot)) \leq y_3(0, \cdot)$.

3 Discretization of the equations

For simplicity, we discuss the discretization in space and time when the cable has a constant length.

3.1 Discretization in space

We propose a space discretization based on a variational formulation of equations (2.1) and (2.2). Consider two appropriate function spaces \mathcal{Y} and \mathcal{T} and the problem: find, for each fixed t , $y(\cdot, t) \in \mathcal{Y}$ and $T(\cdot, t) \in \mathcal{T}$ such that for all $z \in \mathcal{Y}$ and $\tau \in \mathcal{T}$,

$$m_c \int_0^\ell \ddot{y} z + m_f \ddot{y}(0, t) z(0) + \int_0^\ell T y' z' = \int_0^\ell d_c z + d_f z(0) + m_c \int_0^\ell (g - \ddot{u}) z + m_f (g - \ddot{u}) z(0)$$

and

$$\frac{1}{2} \int_0^\ell (|y'|^2 - 1) \tau = 0.$$

A sufficiently smooth solution of this problem satisfies (2.1) and (2.2). We get a discretization of these equations by replacing \mathcal{Y} and \mathcal{T} by some finite element spaces \mathcal{Y}_h and \mathcal{T}_h . For compatibility reasons, the elements of \mathcal{Y}_h must be of higher order than those of \mathcal{T}_h .

To define \mathcal{Y}_h and \mathcal{T}_h , we introduce a grid of $[0, \ell]$ and consider piecewise affine approximations of y and T . The vectors of values approximating y and T at the nodes of the grid are denoted by the same letters y and T . The components of y are computed at each node (except at $s = \ell$, since it is known that $y(\ell, \cdot) = 0$), while the components of T approximate the tension at one node out of two. The spaces \mathcal{T}_h and \mathcal{Y}_h are respectively referred to as P1 and P1-iso-P2 finite element spaces. The discrete variational formulation results in the following index-3 differential-algebraic system of unknowns y , v and T

$$\begin{cases} \dot{y} = v \\ M\dot{v} + R(y)^\top T = B(y, v) \\ C(y) = 0, \end{cases} \quad (3.5)$$

where B is also a function of \dot{u} and \ddot{u} , and $C'(y) = R(y)$.

3.2 Discretization in time

Equation (3.5) is integrated in time using a backward differentiation formula (BDF) scheme (see [1]). The integration interval $[0, t_{\max}]$ is divided in n_t subintervals of constant length dt (the timestep). Let y^i , v^i , and T^i be the approximations of y , v , and T at the times $i dt$, $i = 1, \dots, n_t$. Has to be solved for each i

$$\begin{cases} y^i = dt b_i v^i + \sum_{j=1}^{r_i} a_{i,j} y^{i-j} \\ v^i = dt b_i M^{-1} (B(y^i, v^i) - R(y^i)^\top T^i) \\ \quad + \sum_{j=1}^{r_i} a_{i,j} v^{i-j} \\ C(y^i) = 0, \end{cases} \quad (3.6)$$

where $a_{i,j}$, b_i , and r_i are constants depending on the scheme order, y^0 and v^0 are the initial position and speed y_0 and v_0 .

We suppose that the number of timesteps is fixed to n_t , so that to minimize the total time of the maneuver $t_{\max} = n_t dt$, one has to minimize the value of dt .

4 Optimization techniques

In this section, we denote by $x = (Y, U) \in \mathbb{R}^n$ the vector of variables to optimize. It is formed of the state variables $Y = (y, \dot{y}, T, \kappa) \in \mathbb{R}^{m_E}$ and control variables $U = (\dot{u}, dt, \ell) \in \mathbb{R}^{n-m_E}$. Then, equations (3.6) can be written $c_E(x) = 0$, where c_E is some nonlinear function from \mathbb{R}^n to \mathbb{R}^{m_E} . Similarly, the inequality constraints acting on the state and control variables can be written $c_I(x) \leq 0$, for some function $c_I : \mathbb{R}^n \rightarrow \mathbb{R}^{m_I}$. With this notation, the optimization problem can be written

$$\begin{cases} \min f(x) \\ c_E(x) = 0 \\ c_I(x) \leq 0, \end{cases} \quad (4.7)$$

where the criterion is simply $f(x) = dt$.

This problem is first transformed in a canonical form by introducing slack variables $s \in \mathbb{R}^{m_I}$ and by writing the inequality constraints as $c_I(x) + s = 0$ and $s \geq 0$. It is known that if x is a regular solution, there exist Lagrange multipliers $\lambda_E \in \mathbb{R}^{m_E}$ and $\lambda_I \in \mathbb{R}^{m_I}$ associated with the constraints of (4.7), such that there holds

$$\begin{cases} \nabla f(x) + A_E(x)^\top \lambda_E + A_I(x)^\top \lambda_I = 0 \\ S \lambda_I = 0 \\ c_E(x) = 0 \\ c_I(x) + s = 0 \\ (s, \lambda_I) \geq 0, \end{cases} \quad (4.8)$$

where $A_E(x) = c'_E(x)$ is the $m_E \times n$ Jacobian of the equality constraints, $A_I(x) = c'_I(x)$, and S is the diagonal matrix formed with the components of s . The first equation in (4.8) is conveniently written $\nabla_x \mathcal{L}(x, \lambda) = 0$, where $\mathcal{L}(x, \lambda) = f(x) + \lambda^\top c(x)$ is the Lagrangian of the problem, $\lambda = (\lambda_E, \lambda_I)$, and $c = (c_E, c_I)$.

So-called *primal-dual nonlinear interior point methods* solve approximately a perturbed version of the optimality system (4.8), namely

$$\begin{cases} \nabla_x \mathcal{L}(x, \lambda) = 0 \\ S \lambda_I = \mu e \\ c_E(x) = 0 \\ c_I(x) + s = 0 \\ (s, \lambda_I) > 0, \end{cases} \quad (4.9)$$

for a sequence of perturbation parameters $\mu > 0$ converging to zero. In (4.9), $e = (1 \dots 1)^\top$ is the vector of all ones. The advantage of this approach is that (4.9), as opposed to (4.8), is a set of equalities (the positive constraints on (s, λ_I) are in fact easier to handle than non-negativity constraints), without the combinatorial problem of determining which of the variables s_i or λ_i has to vanish, and with a Newton step that is well defined in the neighborhood of a regular solution. On the other hand, several nonlinear systems of that type have to be solved.

Solving (4.9) approximately requires sophisticated numerical techniques, which we briefly describe (see [3] for more details). The basic idea is to compute an appropriate approximation of the Newton direction associated with (4.9). The latter is the solution $d = (dx, ds, d\lambda_E, d\lambda_I)$ of the linear system (we drop the function dependencies for simplicity):

$$\begin{pmatrix} \nabla_{xx}^2 \mathcal{L} & 0 & A_E^\top & A_I^\top \\ 0 & \Lambda_I S^{-1} & 0 & I \\ A_E & 0 & 0 & 0 \\ A_I & I & 0 & 0 \end{pmatrix} \begin{pmatrix} dx \\ ds \\ d\lambda_E \\ d\lambda_I \end{pmatrix} = - \begin{pmatrix} \nabla_x \mathcal{L} \\ \lambda_I - \mu S^{-1} e \\ c_E \\ c_I + s \end{pmatrix},$$

where Λ_I is the diagonal matrix formed with the elements of λ_I . Since the matrix above uses the Hessian of the Lagrangian $\nabla_{xx}^2 \mathcal{L}$, second derivatives of f and c must be computed or approximated. In our algorithm, only Hessian-vector products $(\nabla_{xx}^2 \mathcal{L})v$ are required.

Close to a solution of (4.9), Newton's direction d is very efficient, but far away it may be inadequate. To improve d , its component in the space tangent to a constraint manifold is approached by solving a reduced form of the linear system above by truncated conjugate gradient iterations. Truncation occurs on several circumstances, but certainly before the possible nonconvexity of the problem is detected.

The above strategy has a second advantage. The modified Newton direction \tilde{d} is a descent direction of the merit function in the variable $z = (x, s, \lambda_E, \lambda_I)$

$$\Theta(z) = f(x) - \mu \sum_{i=1}^{m_I} \log s_i + \lambda_I^\top c_I(x) - \mu \sum_{i=1}^{m_I} \log(\lambda_i s_i) + \sigma_E \|c_E(x)\| + \sigma_I \|c_I(x) + s\|.$$

For judicious positive values of σ_E and σ_I , adapted by the algorithm, the solutions of (4.9) are minimizers of Θ (exact penalty property). Therefore it makes sense to force the decrease of Θ along the direction \tilde{d} , which gives a step-size $\alpha > 0$. Then, z is updated by $z_+ = z + \alpha \tilde{d}$. By this technique, one can force the convergence of the iterates from remote starting points.

5 Numerical experiments

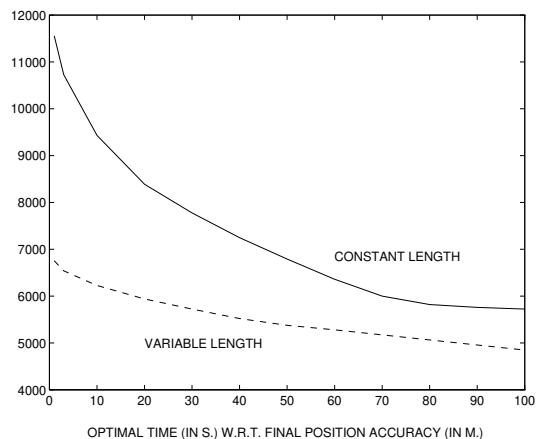
In the experiments, we assume that in a prospecting campaign a rectangular subsea area is explored rows by rows with the cable-vehicle system in steady state. When the vehicle leaves a row, it is desired that it enters the next row as fast as possible. The aim is therefore to make a U-turn in a minimum time. This problem can be set in the framework introduced in the previous sections.

Here are the data of the experiments. The distance between two successive rows is 500 m. The vessel has a nominal speed of 1 m/s, which must be maintained between 0.5 and 1.5 m/s. The cable weighs $m_c = 0.986$ kg/m, it has a nominal and maximal length of 4000 m and 5000 m respectively, and it can be wound and unwound at 1 m/s at most. The vehicle mass is $m_f = 1500$ kg. The drag coefficients c_n , c_t , c_h , and c_z are estimated by the formulae $c_n = \rho D C_n / 2$,

$c_t = \rho D C_t / 2$, $c_h = \rho S_h C / 2$, and $c_z = \rho S_z C / 2$ (ρ : water mass per unit volume, D : cable diameter, S_h : horizontal cross-section area, S_z : vertical cross-section area, and $C_n = 2.3$, $C_t = C_n / 100$, C are empirical drag coefficients). We took $c_n = 23$ kg/m², $c_t = 0.23$ kg/m², and $c_h = c_z = 500$ kg/m.

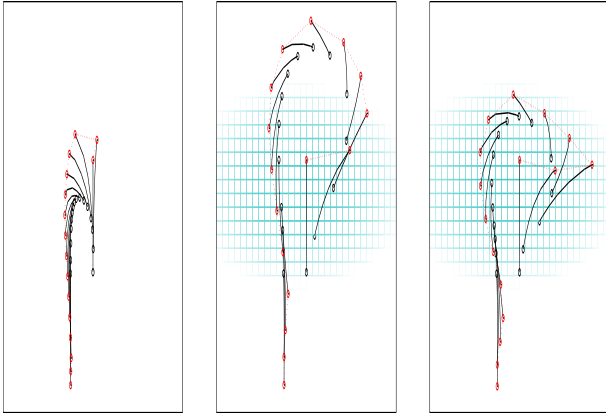
To analyze this situation and the possibilities of the optimization algorithm, we have developed a software in Matlab. For the results below, the discretization is made using 8 equidistant points in space (for the position y) and 15 timesteps. Compared to the steady state solution, which can be computed very accurately by integrating an ordinary differential equation, this discretization in space gives already a rather good approximation. For example, for a cable 4000 m long at 1 m/s, the error on the position of the vehicle is 9 m.

The constraints at the end of the U-turn require that the cable be in a tube of specified radius r_y around the steady state position and that the velocity be between 0.9 and 1.1 m/s. We have compared the optimal times for values of r_y ranging between 1 m and 100 m and for fixed or variable length cables. The results are given in the figure below.

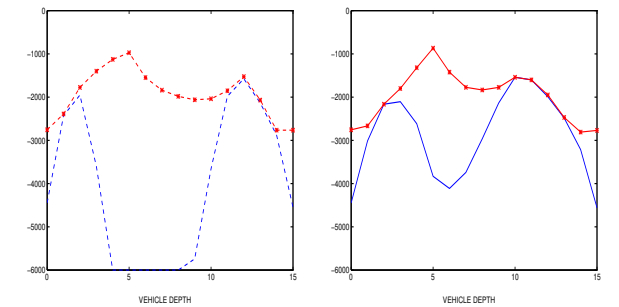
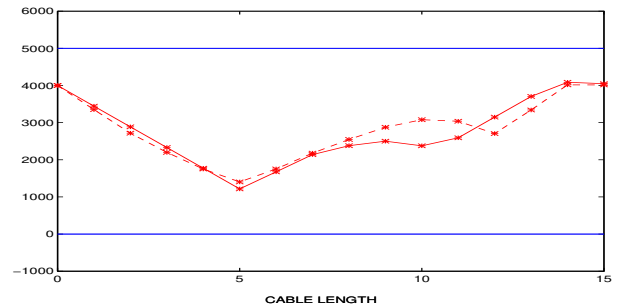
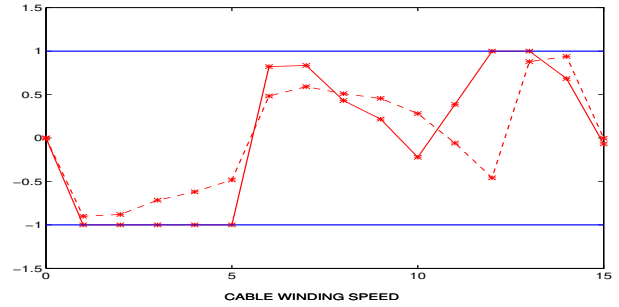
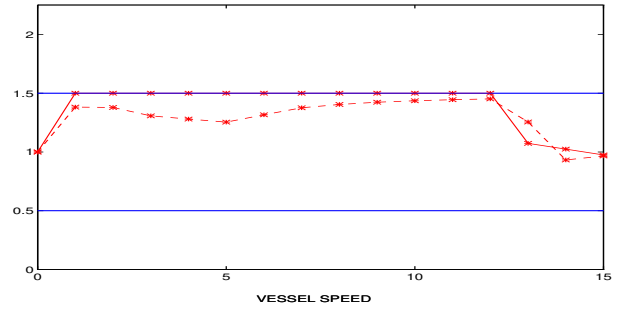
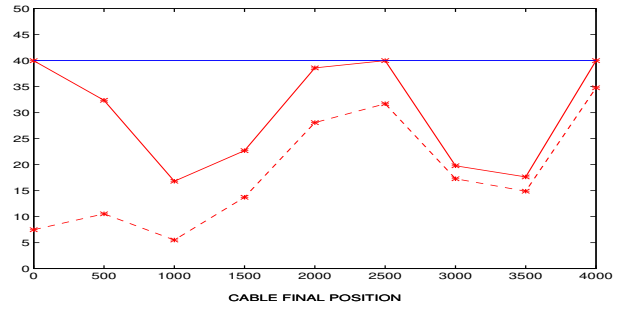
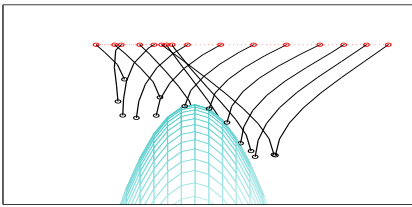
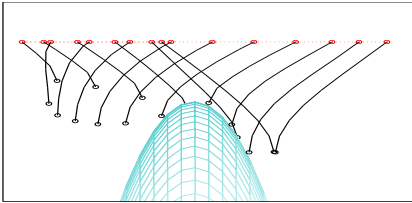
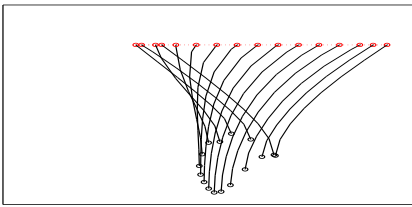


Not surprisingly, more precise the final position must be, more time the maneuver takes, and the dependency is monotone. The time of the U-turn is also longer for a constant length cable, since there is one degree of freedom less than for variable length cables. According to the figure, the possibility to wind the cable during the maneuver is all the more beneficial when high precision is required on the final position. For example, for a precision of 1 m, 40 % of the time is saved when the length of the cable may vary.

In the following tests, the final position tolerance is $r_y = 40$ m, that is to say 1% of the cable nominal length. We represent, on the left and on the right of the figure below, the optimal vessel-cable-vehicle trajectories in the absence or presence of a sea bed relief. The optimal trajectories are seen from above. They correspond to solutions to the optimality system (4.8). The figure in the middle is the solution of (4.9) with the perturbation parameter $\mu = 10^4$.



The respective optimal times are 5520 s, 10820 s, and 8350 s. We show below, from top to bottom, these trajectories seen from the left hand side.



One can observe that the need to avoid the underwater obstacle results in very different optimal trajectories. These pictures also highlight the fact that solutions to (4.9) may vary significantly when μ decreases to zero.

This is confirmed by the figures hereafter, which are all related to the test with obstacle. They successively depict, with their bounds, the distance between the cable nodes and their prescribed position, the vessel speed, the cable winding speed, and the cable length, for solutions to (4.9) with $\mu = 10^4$ (dashed line) and $\mu = 0$ (solid line). The last two pictures give the towfish depth (top line) and the relief of the sea bed along its trajectory (bottom line), for $\mu = 10^4$ (on the left) and $\mu = 0$ (on the right).

Observe that these constraints are inactive when μ is positive. This makes the perturbed optimality conditions (4.9) easier to solve than the optimality conditions (4.8). Moreover, the pictures suggest that allowing for variable length cables not only offers a reduction of the total time, but is also an efficient way of avoiding obstacles.

6 Conclusion

The optimization algorithm presented above is to be included into an integrated computer-aided piloting system for deep-towed/deep-tethered vehicles. It concerns not only U-turn maneuvers but also short transits between investigated areas, surveys along non-straight routes, etc. Simultaneously, Ifremer has started operating a new Ultra Short Base Line acoustic positioning system. This system, recently developed by Thomson Marconi Sonars is accurate to within 1% of the range. It will provide the data necessary to identify current-induced biases in the cable model. It also opens the possibility for a closed-loop adjustment of the preshaped ship trajectory. Further work will focus on taking ship maneuverability constraints into account and interfacing with ship's dynamic positioning systems.

The algorithm presented in this paper, though it can be considered as a prototype software element, appears sufficiently promising in terms of time-effectiveness and robustness. This development is a major step towards the achievement of the complete system.

References

- [1] K.E. Brenan, S.L. Campbell, L.R. Petzold (1989). *Numerical Solution of Initial-Value Problems in Differential-Algebraic Equations*. North-Holland, New-York. [3](#)
- [2] R.H. Byrd, J.Ch. Gilbert, J. Nocedal (2000). A trust region method based on interior point techniques for nonlinear programming. *Mathematical Programming*, 89, 149–185. [\[doi\]](#). [1](#)
- [3] L. Chauvier (2000). *Commande Optimale d'Engins Sous-Marins avec Contraintes*. Thèse de doctorat, Université Paris I (Panthéon-Sorbonne). [1](#), [4](#)
- [4] G. Damy, M. Joannides, F. Le Gland, M. Prevosto, R. Rakotozafy (1994). Integrated short term navigation of a towed underwater body. In *Proceedings of the IEEE Conference "Oceans'94"*. Brest, France. [2](#)
- [5] F. Hover (1993). *Methods for Positioning Deeply-Towed Underwater Cables*. SdD Thesis, WHOI/MIT. [1](#)
- [6] D. Marichal, B. Dassonville, O. Lefort (1987). Étude dynamique des systèmes sous-marins remorqués à l'aide de câbles de longueur variable. Association Technique Maritime et Aéronautique, Session 1987, 47 rue Monceau, 75008 Paris. [2](#)
- [7] J.D. Mudie, K.A. Kastens (1980). Computer aided piloting of a deeply towed vehicle. *Ocean Engineering*, 7, 743–754. [1](#)
- [8] N. Pichon (1997). *Modélisation, Simulation et Commande Optimale pour le Remorquage d'Engins Sous-Marins Profonds*. Thèse de doctorat, Université Paris IX (Dauphine). [1](#)